A Fourier Split-Step Based Wide-Angle Three-Dimensional Vector Parabolic Wave Equation Algorithm Predicting the Field Strength Over Flat and Irregular Forest Environments

Hafiz Faiz Rasool, Xiao-Min Pan*, and Xin-Qing Sheng

Center of Electromagnetic Simulation, School of Information and Electronics
Beijing Institute of Technology, Beijing, 100081, People's Republic of China
hafiz@bit.edu.cn, *xmpan@bit.edu.cn, xsheng@bit.edu.cn,

Abstract ─ This paper provides the analysis of radio wave propagation prediction over flat and irregular forest environments. A three-dimensional vector parabolic wave equation (3DPE) method is used to calculate the field strength due to the forest on a lossy ground. Forest terrains are equivalent to a series of absorbing blocks arranged along the direction of propagation. Under the assumption of forwarding propagation, a 3DPE is derived and the Fourier split-step based PE (SSPE) method is adopted to march the potentials from one aperture plane to the next. A Tukey window function is used to attenuate the fields smoothly at the upper boundary without reflections. Finally, the simulation results are compared with the analytical methods presented in the literature. The simulation results have shown the validity of the proposed algorithm.

Index Terms ─ Forest terrains, parabolic wave equation, radio wave propagation, split-step parabolic equation method, wave propagation prediction.

I. INTRODUCTION

Wave propagation is an important phenomenon in many applications. The analysis of ground wave propagation depends on the characteristics of the lower layer of the atmosphere and the terrain over which the wave propagates. Electromagnetic waves (EM) are affected by the propagation environments due to change in temperature, pressure, and humidity. Non-flat terrains, buildings, trees, and mountains also disturb the waves and lead to the variation of field strength [1].

In the rural and suburban areas, the forest is an important factor affecting the radio wave propagation over a long distance. Due to the absorption and scattering properties of the trees, the attenuation and phase shift of signals mostly happen which affects the target identification and other wireless communications greatly [2]. Therefore, it has very important practical application value to study the forest effect on wave propagation. Several empirical and deterministic methods have been presented in the literature for propagation analysis [3-5]. Empirical models require less computational effort, but these models do not consider the details of the local terrain topography. On the other hand, deterministic models require a vast amount of data regarding terrain profile, more computational resources and are more accurate than the empirical models [6,7]. The approaches based on parabolic equation (PE) are another way to predict the wave behavior, it was first introduced by Leontovich and Fock in the 1940s [8]. Later, it has become a popular method in EM wave propagation modeling. The PE method gets the environmental parameters as input, it accepts different boundary conditions (BCs) and allows to use different types of antenna patterns [9, 10]. Due to these characteristics, the PE method nowadays is a preferred method for solving radio wave propagation problems [11-13]. There are many numerical methods available to solve parabolic type wave equations such as Finite Difference method, Finite Element method, and Method of Moment in the literature [14], but the SSPE method is more suitable to solve PE for long-range propagation. This method is highly efficient both in memory usage and in runtime [15-19].

In recent years, many scholars have done some research on radio wave propagation problems in forest environments using PE method [20-25]. Still, these models are 2D in nature either it is based on scalar formulations or it has been designed for a small area.

The goal of this paper is to introduce the 3DPE method in a forest environment based on SSPE method, to predict the wave propagation due to the forest over a large area. It is shown that the 3DPE model can formulate both vertical and lateral wave propagation into account. The basic formulation of the 3DPE is discussed briefly, which is followed by the explanation of the SSPE method and the corresponding numerical implementation.

This paper is organized into five sections as follows. In the next section, the basic formulation of the wide-angle 3DPE is discussed. Section 3 presents the SSPE

Submitted On: October 24, 2018
Accepted On: April 3, 2019

solution to the proposed algorithm. In Section 4, numerical implementation steps are discussed such as initial field, domain discretization, boundary conditions, etc. Section 5 presents the simulation results and comparisons with the results presented in the literature.

II. FORMULATION OF THE 3DPE

In cartesian coordinates (*x*, *y*, *z*), considering the propagation in a homogeneous medium with refractive index *n* and supposing a time convention $e^{-i\omega t}$, where $\omega = 2\pi f$ is the radian frequency at the frequency *f*. Supposing that the fields are excited by a vertically polarized (z-oriented) sources at a given range x_0. The electric current density of the distributed source located at $x = 0$ is assumed to be $\vec{J}_z = I_0 l \delta(x)\delta(y) f^e(y,z)$, where $f^e(y,z)$ is the 2D Gaussian function, $I_0 l$ is the current moment and $\delta(\cdot)$ denote the unit delta function, respectively. Expressing the fields in terms of two z-oriented potentials, it is easy to see from Maxwell's equations that [26]:

$$E_z^e = \frac{i\eta_0}{n^2 k_0}\left(\frac{\partial^2}{\partial z^2} + k_0^2\right)\psi^e = E_z, \tag{1}$$

$$H_z^m = \frac{i}{\eta_0 k_0}\left(\frac{\partial^2}{\partial z^2} + k_0^2\right)\psi^m = H_z, \tag{2}$$

where ψ^e and ψ^m are the scalar potentials arising from the electric and magnetic currents, respectively. The superscripts "*e*" and "*m*" identify the sources (electric or magnetic) that give rise to the potentials and fields. The wavenumber and intrinsic impedance in free space are denoted by k_0 and η_0, respectively. The total fields $\vec{E} = \vec{E}^e + \vec{E}^m$ and $\vec{H} = \vec{H}^e + \vec{H}^m$ are decomposed in terms of a TEz mode and a TMz mode with constituent fields [27]:

$$\begin{aligned} E_x^e &= \frac{i\eta_0}{n^2 k_0}\frac{\partial^2 \psi^e}{\partial x \partial z}, \quad H_x^e = \frac{\partial \psi^e}{\partial y}, \\ E_y^e &= \frac{i\eta_0}{n^2 k_0}\frac{\partial^2 \psi^e}{\partial y \partial z}, \quad H_y^e = -\frac{\partial \psi^e}{\partial x}, \end{aligned} \tag{3}$$

$$\begin{aligned} E_x^m &= -\frac{\partial \psi^m}{\partial y}, \quad H_x^m = \frac{i}{\eta_0 k_0}\frac{\partial^2 \psi^m}{\partial x \partial z}, \\ E_y^m &= \frac{\partial \psi^m}{\partial x}, \quad H_y^m = \frac{i}{\eta_0 k_0}\frac{\partial^2 \psi^m}{\partial y \partial z}. \end{aligned} \tag{4}$$

Using this representation of the fields, and in a source-free region $\psi = \psi^e + \psi^m$ and thus from the Helmholtz equation, PE can be obtained as [9, 11]:

$$\left[\nabla^2 + k_0^2 n^2\right]\psi = 0, \tag{5}$$

where ∇^2 is the Laplacian operator and replacing ψ with $e^{-ik_0 x}\psi$, the wide-angle 3DPE can be obtained as [28, 29]:

$$\frac{\partial \psi}{\partial x} = ik_0(n-2) + i\sqrt{k_0^2 + \left(\frac{\partial^2}{\partial y^2} + \frac{\partial^2}{\partial z^2}\right)}\psi. \tag{6}$$

III. FOURIER SPLIT-STEP ALGORITHM

In numerical analysis, the Fourier split-step method is a type of pseudo-spectral method used to solve highly nonlinear time-dependent partial differential equations in engineering and physics applications [30]. We are briefly explaining this method as in [31]. Starting from (6) and introducing the two operator's *M* and *N* as:

$$\frac{\partial \psi}{\partial x} = \left[M(x,y,z) + N(y,z)\right]\psi, \tag{7}$$

$$M = ik_0(n-2), \quad N = i\sqrt{k_0^2 + \left(\frac{\partial^2}{\partial y^2} + \frac{\partial^2}{\partial z^2}\right)}. \tag{8}$$

Supposing that Δx is the range incremental step size, then the split-step solution at $x + \Delta x$ can be written as:

$$\psi(x+\Delta x, y, z) = e^{\int_x^{x+\Delta x} M(x,y,z)dx + \int_x^{x+\Delta x} N(y,z)}\psi(x,y,z), \tag{9}$$

the operator $[M(x,y,z) + N(y,z)]$ does not commute in this integral. With the assumption that the refractive index *n* is slowly varying at each small range step Δx in yz-plane then it can be formally expressed as [32]:

$$\psi(x+\Delta x, y, z) \simeq e^{M\Delta x + N\Delta x} = e^{M\Delta x} e^{N\Delta x}\psi(x,y,z). \tag{10}$$

In the approximated exponentials, the term $e^{M\Delta x}$ is a multiplication operator which can be solved numerically easily, while the exponential operator $e^{N\Delta x}$ is a differential operator which can be solved with the help of Fourier transform. Let $\psi = F_2^{-1}\left[F_2(\psi)\right]$, similarly,

$$e^{N\Delta x}\psi(x,y,z) = F_2^{-1}\left[F_2\left\{e^{N\Delta x}\psi(x,y,z)\right\}\right], \tag{11}$$

where F_2 and F_2^{-1} denote the 2D Fourier transforms and it's inverse Fourier transforms respectively. Equation (10) can be written as:

$$\psi(x+\Delta x, y, z) = e^{M\Delta x} F_2^{-1}\left[F_2\left\{e^{N\Delta x}\psi(x,y,z)\right\}\right], \tag{12}$$

using (8) and (12), one can get the SSPE solution for the wide-angle 3DPE as [29]:

$$\psi(x+\Delta x, y, z) = e^{ik_0\Delta x(n-2)} \times F_2^{-1}\left[e^{ik_x\Delta x} F_2\left\{\psi(x,y,z)\right\}\right], \tag{13}$$

where $k_x = \sqrt{k_0^2 - k_y^2 - k_z^2}$ is the wavenumber along the range axis for a plane wave traveling in the (k_y, k_z) direction. Here, k_y and k_z are the Fourier transform domain variables. It is the solution of an electromagnetic wave when the refractive index *n* is varying slowly at each small range step Δx in a homogeneous medium.

IV. NUMERICAL IMPLEMENTATION

In this section, we have discussed some important implementation steps for the numerical simulation of the proposed algorithm.

A. Boundary conditions

The PE model requires BCs to avoid the reflection at $z = \pm z_{\max}$ and $y = \pm y_{\max}$ along the *y* and *z* axes, respectively. An absorbing boundary condition is used in this paper as:

$$W(j,k) = w(j) \cdot w(k), \quad j = 1: N_y, k = 1: N_z, \qquad (14)$$

where *w* is the Tukey window function, with $N(N_y, N_z)$ being the Fourier transform size. [33]. Therefore, the potential at (*x*, *y*, *z*) is finally computed as:

$$\psi(i\Delta x, j\Delta y, k\Delta z) = \psi(i\Delta x, j\Delta y, k\Delta z) \cdot W(j,k). \qquad (15)$$

Besides, the forest terrain surface is assumed to be a lossy and trees are equivalent to a series of absorbing blocks arranged along the direction of propagation.

B. Domain discretization

The domains are truncated at $\pm z_{\max}$ and $\pm y_{\max}$ (maximum distance along the *y*– and *z* directions). The step size along *x*, *y*, and *z* directions defined as Δx, Δy and Δz respectively. Maximum altitude $z_{\max}$ is determined from the source/observation requirements to minimize the aliasing effects. Once $z_{\max}$ or $y_{\max}$ is decided then $k_{y\max}$ and $k_{z\max}$ are calculated from the Nyquist criterion as $z_{\max} \times k_{z\max} = \pi N$ and $y_{\max} \times k_{y\max} = \pi N$ at the same time. As $k_{y\max} = k_0 \sin\theta_{\max}$ and similarly, $k_{z\max} = k_0 \sin\theta_{\max}$, where $\theta_{\max}$ is the maximum allowable propagation angle [11]. As $\Delta z = z_{\max} / N$ and $\Delta y = y_{\max} / N$, and if $\Delta l = \sqrt{\Delta y^2 + \Delta z^2}$ then we have, $\Delta l \le \pi / k_0 \sin\theta_{\max}$ to predict the maximum propagation angle. The choice of the incremental range Δx is provided by the user and it can be as large as λ since $\psi(x, y, z)$ varies slowly along *x* in the yz-plane [26].

C. Initialization of the algorithm

The numerical solution of SSPE algorithm usually starts with the given initial potential. It relates to the field radiated by the transmitting antenna. The transformed potential provides the initial potential for the beginning of the algorithm. In this work, we generate it by a vertically polarized current source with a Gaussian aperture distribution whose electric current is I_0 and length *l*, which is given as [26]:

$$\psi^e(0^+, y, z) \approx \frac{iI_0 l}{2k_0} f^e(y, z), \qquad (16)$$

$$f^e(y,z) = \frac{1}{\sigma_z\sqrt{2\pi}} e^{-\frac{(z-H_t)^2}{2\sigma_z^2}},$$

where H_t represents the height of the transmitting antenna and σ_z is the source standard deviation used to set 3 dB elevation beamwidth of transmitting antenna. Because the magnetic current is assumed to be zero here, therefore the initial condition for ψ^m is simply $\psi^m(0^+, y, z) = 0$. The transformed potential $\tilde{\tilde{\psi}}(0^+, k_y, k_z)$ can be easily determined using Fourier transform of the current source with respect to *z*, and $\tilde{\tilde{\psi}}$ is the 2D-Fourier transform of the aperture field [26]:

$$\tilde{\psi}(0^+, 0^+, k_z) = F\left[f^e(y,z) \right] = e^{-ik_z H_t} e^{-k_z^2 \sigma_z^2/2}. \qquad (17)$$

The initial potential can be defined as a column vector with N_z elements along the z-axis, again as $\vec{J}_z$ is independent of *y* one can repeat the column of $\tilde{\psi}\left(0^+, 0^+, k_z\right) N_y$ times along the y-axis. In this way, a 2D initial potential $\tilde{\tilde{\psi}}\left(0^+, k_y, k_z\right)$ can be obtained with $N_y \times N_z$ dimension. In order to apply the impedance surface BCs on a forest terrain the image theory is applied, implying that the fields and their corresponding potentials are represented in terms of odd and even parts. This infers that the Gaussian source representation is equally split into its even and odd components, $\left(\tilde{\psi}_e\right)$ and $\left(\tilde{\psi}_o\right)$, respectively:

$$\begin{aligned} \tilde{\psi}_e(0^+, k_y, k_z) &= e^{-k_z^2 \sigma_z^2/2} \cos(k_z H_t), \\ \tilde{\psi}_o(0^+, k_y, k_z) &= -ie^{-k_z^2 \sigma_z^2/2} \sin(k_z H_t). \end{aligned} \qquad (18)$$

Neglecting the surface waves in the far zone, under this approximation the initial field is the 2D Fourier transform of the aperture field $\tilde{\tilde{\psi}}$ that satisfies the impedance boundary over the ground as [26]:

$$\begin{aligned} \tilde{\tilde{\psi}}(x, k_y, k_z) = \int_{z'=0}^{+\infty} \int_{y'=-\infty}^{+\infty} \psi(x, y', z') e^{-ik_y y'} \\ \cdot \left[e^{-ik_z z'} + \Gamma(k_z) e^{ik_z z'} \right] dy' dz', \end{aligned} \qquad (19)$$

where $\Gamma(k_z)$ is the reflection coefficient of the plane waves over an impedance terrain surface with impedance *Z* for TMz and TEz modes, which is given as:

$$\begin{cases} \Gamma_{\mathrm{TM}_z}(k_z) = \dfrac{k_z - Zk_0}{k_z + Zk_0} \\ \Gamma_{\mathrm{TE}_z}(k_z) = \dfrac{Zk_z - k_0}{Zk_z + k_0} \end{cases}, \qquad (20)$$

the normalized complex impedance of the terrain surface is given as $Z = 1\Big/\sqrt{\varepsilon_{rf} + \dfrac{i\sigma_f}{\omega\varepsilon_0}}$, where σ_f is the conductivity and ε_{rf} is the relative permittivity of the forest terrain, respectively [26, 34]. Actually, Eq. (19) is not a 2D Fourier transform, but a complicated double integration. While it can be evaluated easily with the help of fast Fourier transform (FFT) instead of evaluating double integrals. For example, the potentials are represented in terms of odd and even parts $\psi = \dfrac{\psi_e + \psi_o}{2}$. Assuming that $A = e^{-ik_z z'}$ and $B = e^{ik_z z'}$ then the integral part corresponds to z in (19) can be written as:

$$\int_{z'=0}^{+\infty} \left[A + \Gamma(k_z)B\right]\psi(x, y', z')dy'dz'. \tag{21}$$

In order to apply the FFT, changing the limit of integration from 0 to ∞ to $-\infty$ to ∞ [35]. If we add $\psi_e(x, y', z')$ and $\psi_o(x, y', z')$ together for z > 0 and z < 0 we will get back the total field ψ. In this way, we can obtain Eq. (22) by prolix deduction as given below:

$$\begin{aligned}&\int_{z'=0}^{+\infty} \left[A + \Gamma(k_z)B\right]\psi(x, y', z')dy'dz', \\ &= \int_{-\infty}^{+\infty} \frac{1+\Gamma(k_z)}{2} A\psi_e(x, y', z')dz' \\ &\qquad + \int_{-\infty}^{+\infty} \frac{1-\Gamma(k_z)}{2} A\psi_o(x, y', z')dz',\end{aligned} \tag{22}$$

substituting (22) into (19) and thus, the initial potential $\tilde{\tilde{\psi}}(0^+, k_y, k_z)$ can be obtained for the beginning of the algorithm as:

$$\begin{aligned}\tilde{\tilde{\psi}}(0^+, k_y, k_z) &= \frac{1+\Gamma(k_z)}{2}\tilde{\tilde{\psi}}_e(0^+, k_y, k_z) \\ &\quad + \frac{1-\Gamma(k_z)}{2}\tilde{\tilde{\psi}}_o(0^+, k_y, k_z).\end{aligned} \tag{23}$$

After initializing the potentials $\psi(0^+, y, z)$ at $x = 0^+$ the field values at $x(0^+ + \Delta x)$ are computed by applying the propagator $e^{ik_x \Delta x}$ to the Fourier transformed field $\tilde{\psi}(0^+, k_y, k_z)$. Hence, obtaining the field values at the successive location $x + \Delta x$ by an inverse Fourier transform as can be seen in Eq. (24) the double integration corresponds to an inverse Fourier transform where k_y and k_z are the transformation domain variables:

$$\psi(x + \Delta x, y, z) = \frac{1}{4\pi^2}\int_{-\infty}^{+\infty}\int_{-\infty}^{+\infty} e^{ik_x \Delta x}\tilde{\tilde{\psi}}(x, k_y, k_z)e^{i(k_y y + k_z z)}dk_y dk_z, \tag{24}$$

and thus, it can be solved via Split-Step Fourier algorithm which consists of a succession of Fourier and inverse Fourier transforms obtained by FFT and inverse FFT, respectively. Equations (19) and (24) are used for both ψ^e and ψ^m with the appropriate value of $\Gamma(k_z)$ chosen from (20).

V. SIMULATION RESULTS

In this section, the simulation results are presented to check the validity of the proposed algorithm. In order to validate the proposed algorithm, the simulation results are compared with the results presented by Janaswamy as Fig. 11 in [26]. Related studies can also be found in [35]. Figure 1 shows the propagation factor (PF) versus the receiver height (H_r) when a PEC knife edge is placed over the flat terrain between the transmitter and receiver as shown in Fig. 1 inset.

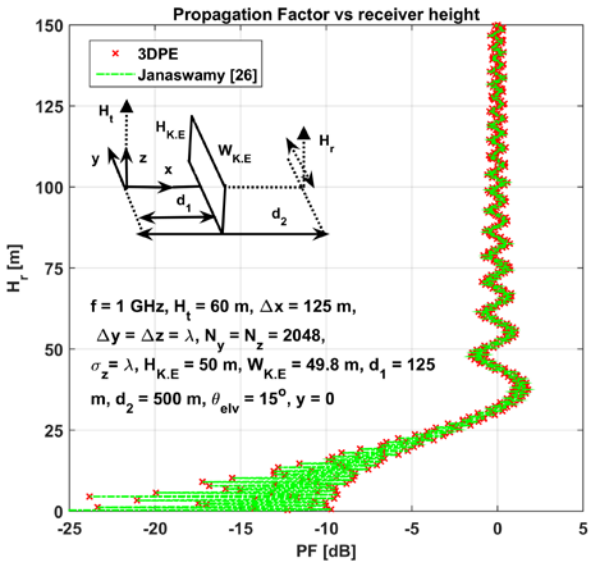

Fig. 1. Propagation factor versus vertical displacement behind a finite absorbing screen (a single knife-edge) as Fig. 11 in [26].

The knife-edge's height $(H_{K.E})$ and width $(W_{K.E})$ are 50 m (meters) and 49.8 m, respectively. The distance between the transmitter and receiver is 500 m, the distance between the transmitter and the PEC knife edge is $d_1 = 125$ m, and the distance between the knife edge and the receiver is 375 m, respectively. The field is computed at $x = x_{\max}$. Other parameters are shown in Fig. 1 inset. Compared with the reference model, the proposed model had an excellent agreement with the results presented in [26] which shows the validity of the proposed algorithm.

All the simulations were realized using a 3.4 GHz Core i7-7600 CPU workstation, 32 GB RAM. Computational time and memory used by the proposed model at different range step sizes are shown in Table 1.

Table 1: Computational time and RAM consumption (Dell 3.4 GHz Core i7-7600 CPU workstation, 32 GB RAM)

No.	Δx (m)	Ny = Nz	RAM (MB)	Time (s)
1	25	1024	626.4	28.47
2	50	1024	627.1	14.35

The second test is related to the field strength prediction over the rows of trees with uniform heights and spacing arranged along the direction of propagation on flat terrain. Field strength prediction due to the forest with non-uniform heights and equal spacing arranged along the direction of propagation on flat terrain is also presented in Fig. 4, and the last example is related to the field strength prediction due to the forest placed over three triangular-shaped mountains.

The simulation results presented in Fig. 3, Fig. 4, and Fig. 5 are compared with the analytical method namely, 3D Ray tracing method. 3D Ray tracing method is successfully applied in propagation modeling through open and closed environments, that may serve as a reference and perform validation, verification, and calibration (VV&C) [36, 37].

Figure 2 shows the geometry of the forest terrain placed in the yz-plane along the direction of propagation between the transmitter and receiver, where F_w is the forest's width and F_h is the forest's height, respectively.

Figure 3 (top) shows the geometry of the flat-shaped forest. The rows of trees with uniform heights (16 m) and separation distance (50 m) on the simulation range of 5 kilometers (km) are considered over the flat earth. The transmitting and receiving antennas are placed at the height of 16 m with 15º propagation angle in the paraxial direction. The operating frequency is considered at 900 MHz. Other operational parameters in all examples are assumed as $\Delta y = \Delta z = \lambda$, $N_y = N_z = 1024$, σ_f = 0.1 mS/m, and $\varepsilon_{rf} = 1.1$, respectively. The effect on the field strength in the presences of rows of trees on flat terrain at $F_w = 200$ m is evaluated as shown in Fig. 3 (middle) and (bottom). We can see that in the start of simulation the field values of the 3DPE method and 3D Ray tracing method are very close to the free space value, while the field values due to the 3DPE model rapidly decrease for short distance very close to the transmitter, it is may be due to the paraxial approximation in PE, it is clearly observed in Fig. 3 (bottom).

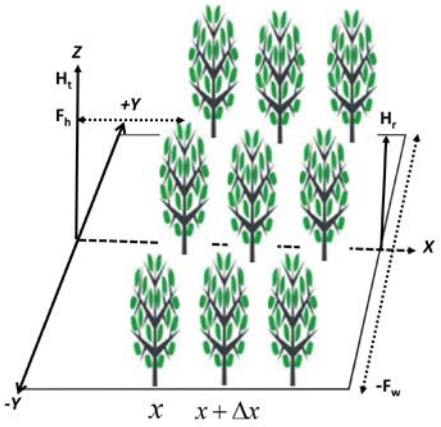

Fig. 2. Rows of trees placed in the yz-plane along the direction of propagation.

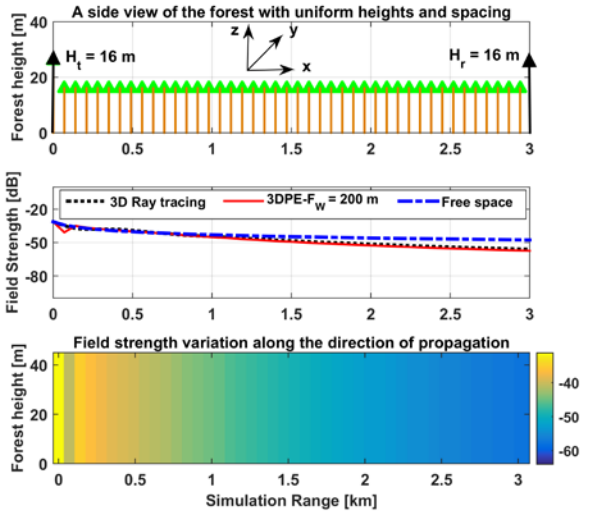

Fig. 3. A side view of the rows of trees with uniform heights and spacing on flat ground in two dimensions (top) [the third dimension, which is the lateral dimension y, is orthogonal to the plane of the paper]. Field strength prediction due to the 3D Ray tracing method and the 3DPE method (middle). Field strength prediction due to 3DPE model at F_w = 200 m (bottom).

The PE method is known to give unreliable solutions very close to the source. The region over which these errors occur is very small indeed (of the order of meters) but because the algorithm is range dependent these errors will propagate. However, preliminary experiments have indicated that the errors do not significantly affect predictions at ranges of interest [38]. The results of [39] indicate that the field degrades for a plane wave incident upon uniform height screens with equal separations as in this paper. We can see that the 3DPE results have good agreement with the 3D Ray

tracing method and the result presented in [39], but the result of the 3D Ray tracing is slightly higher, which implies it overestimates the field amplitude due to the diffracted waves.

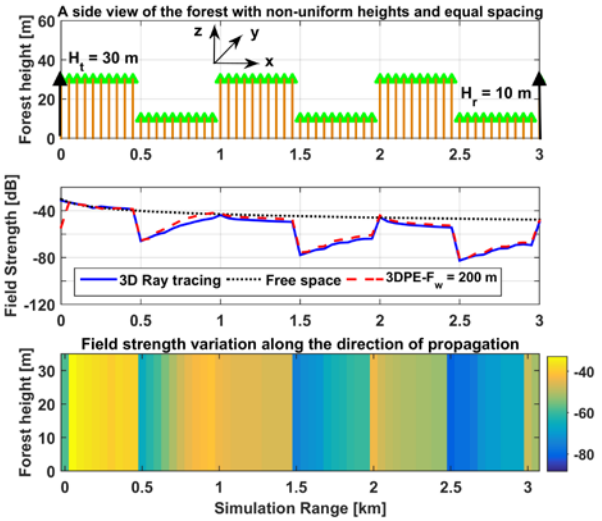

Fig. 4. A side view of the rows of trees with non-uniform heights and equal spacing on flat ground in two dimensions (top) [the third dimension, which is the lateral dimension y, is orthogonal to the plane of the paper]. Field strength prediction due to the 3D Ray tracing method and the 3DPE method (middle). Field strength prediction due to the 3DPE model at $F_w = 200$ m (bottom).

Figure 4 (top) shows the geometry of the flat-shaped forest. The rows of trees with non-uniform heights from 30 m (maximum) to 10 m (minimum) are considered with a separation distance of 50 m on the simulation range of 5 kilometers (km). The transmitting and receiving antennas are placed at the height of 30 m and 10 m respectively, with 15° propagation angle in the paraxial direction. Up to 0.5 kilometers from the transmitter the field values behave like free space and gradually decreasing due to the creeping wave effect, after 0.5 kilometers the field value increases due to the contribution of lateral waves. We can see that the 3DPE results have good agreement with the 3D Ray tracing method, but the results of the 3DPE are slightly higher, due to finite F_w. Therefore, if we increase the F_w, then we expect to see the results of the 3DPE model to agree with 3D Ray tracing results because in 3D Ray tracing method F_w is assumed infinitely long. This is equivalent to the 2DPE model which did not consider the lateral waves. The total field variation is the sum of the direct waves and reflected waves.

Figure 5 shows the geometry of the third test, it is the side view of the forest in a mountainous area with multiple rows of trees with variable heights, equal spacing and variable width distributed on three mountains surfaces. The modeling of the mountain type terrains can be found in [40].

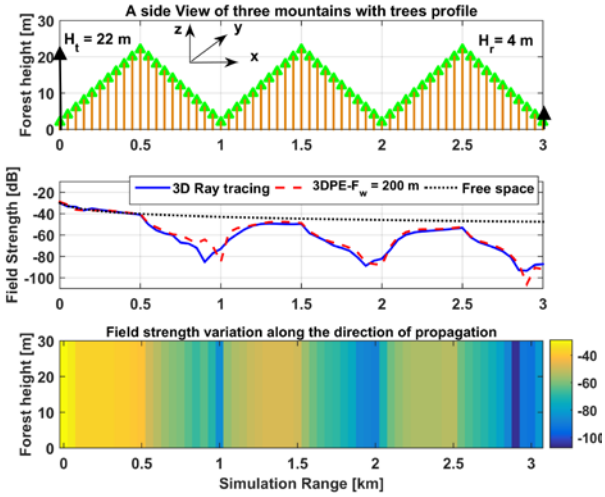

Fig. 5. A side view of the forest placed on the mountainous terrain in two dimensions (top) [the third dimension, which is the lateral dimension y, is orthogonal to the plane of the paper]. Field strength prediction due to the 3D Ray tracing method and the 3DPE method (middle). Field strength prediction due to the 3DPE model at $F_w = 200$ m (bottom).

In Fig. 5, up to 0.5 kilometers from the base station field behaves like free space, then at the first peak of mountain field behaves like a single knife-edge. The field strength minima occur at one kilometer in the 3DPE model. However, the results of 3D Ray tracing show that the ray tracing approach must be improved to handle the transition region effects and the multiple diffraction effects at very small angles.

VI. CONCLUSION

This work has demonstrated the 3DPE model that evaluates the field strength over flat and irregular forest environments. It is shown that the 3DPE model can formulate both vertically and laterally wave propagation effect in a large forest environment. Under the assumption of forwarding propagation, a wide-angle three-dimensional parabolic wave equation (3DPE) is formulated from the Helmholtz equation. The split-step parabolic equation (SSPE) method is adopted to march the potentials from one aperture plane to the next along the direction of propagation. The obtained results have a good agreement with the reference models presented in the literature. The proposed model can be generally used in both national, commercial and military applications for the analysis of radio wave propagation.

ACKNOWLEDGMENT

This work was supported in part by the National Nature Science Foundation of China (NSFC) under Grant No. 61771053 and 61421001.

REFERENCES

[1] H. L. Bertoni, *Radio Propagation for Modern Wireless Systems*. Prentice Hall PTR, New Jersey, 2000.

[2] T. Rappaport, *Wireless Communications Principles and Practice*, 2nd ed., Prentice Hall, New Jersey, 2001.

[3] T. K. Sarkar, Z. Ji, K. Kim, A. Medour, and M. Salazar-Palma, "A survey of various propagation models for mobile communication," *IEEE Antennas Propag. Mag.*, vol. 45, no. 3, pp. 51-82, June 2003.

[4] D. Liao and K. Sarabandi, "Modeling and simulation of near earth propagation in presence of a truncated vegetation layer," *IEEE Trans. Antennas Propag.*, vol. 55, no. 3, pp. 949-957, 2007.

[5] F. Wang and K. Sarabandi, "A physics-based statistical model for wave propagation through foliage," *IEEE Trans. Antennas Propag.*, vol. 55, no. 3, pp. 958-968, 2007.

[6] Y. S. Meng, Y. H. Lee, and B. C. Ng, "Study of propagation loss prediction in forest environment," *Progress in Electromagnetics. Res. B*, vol. 17, pp. 117-133, 2009.

[7] J. Zegarra, "Model Development for Wireless Propagation in Forested Environments," *Thesis and Dissertation Collection*, Naval Postgraduate School, Monterey, California, 2015.

[8] M. A. Leontovich and V. A. Fock, "Solution of the problem of propagation of electromagnetic waves along the earth's surface by the method of parabolic equation," *Academy of Sciences of the USSR: Journal of Physics*, vol. 10, pp. 13-23, 1946.

[9] M. Levy, *Parabolic Equation Methods for Electromagnetic Wave Propagation*. London, IEE Institution of Electrical Engineers, 2000.

[10] I. D. Sirkova and M. Mikhalev, "Parabolic wave equation method applied to the tropospheric ducting propagation problem: A survey," *Electromagnetics*, vol. 26, pp. 155-173, 2006.

[11] G. Apaydin and L. Sevgi, *Radio Wave Propagation and Parabolic Equation Modeling*. Wiley-IEEE Press, 2017.

[12] L. Sevgi, F. Akleman, and L. B. Felsen, "Ground wave propagation modelling: Problem-matched analytical formulations and direct numerical techniques," *IEEE Antennas Propag. Mag.*, vol. 44, no. 1, pp. 55-75, Feb. 2002.

[13] L. Sevgi, C. Uluisik, and F. Akleman, "A Matlab-based two-dimensional parabolic equation radio wave propagation package," *IEEE Antennas Propag. Mag.*, vol. 47, no. 4, pp. 164-175, Aug. 2005.

[14] X. Q. Sheng and W. Song, *Essentials of Computational Electromagnetics*. Singapore, John Wiley & Sons, 2012.

[15] F. Akleman and L. Sevgi, "A novel mom-and sspe-based groundwave-propagation field-strength prediction simulator," *IEEE Antennas Propag. Mag.*, vol. 49, no. 5, pp. 69-82, Oct. 2007.

[16] G. Apaydin and L. Sevgi, "The split-step-fourier and finite-element-based parabolic equation propagation-prediction tools: Canonical tests, systematic comparisons, and calibration," *IEEE Antennas Propag. Mag.*, vol. 52, no. 3, pp. 66-79, June 2010.

[17] G. Apaydın and L. Sevgi, "A novel split-step parabolic equation package for surface wave Propagation prediction along multi-mixed irregular terrain paths," *IEEE Antennas Propag. Mag.*, vol. 52, no. 4, pp. 90-97, Aug. 2010.

[18] O. Ozgun, G. Apaydin, M. Kuzuoglu, and L. Sevgi, "PETOOL: Matlab-based one-way and two-way split-step parabolic equation tool for radiowave propagation over variable terrain," *Computer Physics Communications*, vol. 182, no. 12, pp. 2638-2654, 2011.

[19] P. Zhang, L. Bai, Z. Wu, and L. Guo, "Applying the parabolic equation to tropospheric groundwave propagation: A review of recent achievements and significant milestones," *IEEE Antennas Propag. Mag.*, June 2016.

[20] J. F. De Souza, F. N. B. Magno, Z. A. Valente, J. C. Costa, and G. P. S. Cavalcante, "Mobile radio propagation along mixed paths in forest environment using parabolic equation," *Microwave and Optical Tech. Letters*, vol. 51, no. 4, pp. 1133-1136, Apr. 2009.

[21] P. Holm, G. Eriksson, and P. Kraus., "Wave propagation over a forest edge - parabolic equation modeling vs. measurements," *IEEE Intl. Symp. Radio Comm.*, Portugal, Sep. 2002.

[22] J. F. Souza, Z. A. Valente, F. N.B. Magno, G. P. S. Cavalcante, and J. C. Costa, "Propagation path loss through the Urban foliated semi-confined environment using parabolic equations," *IEEE Intl. Symp. on Spread Spectrum Techniques and Applications*, Brazil, Aug. 2006.

[23] M. Le Palud, "Propagation modeling of VHF radio channel in forest environments," *IEEE Military Communications Conference*, vol. 2, pp. 609-614, Oct. 2004.

[24] J. Guo, J. Wang, P. Liu, and Y. Long, "Fourier split-step parabolic equation solution of wave propagation over forest edge," *2008 Intl. Conference on Microwave and Millimeter Wave Tech.*, Nanjing, China, 21-24 Apr. 2008.

[25] V. A. Permyakov, M. S. Mikhailov, and E. S. Malevich, "Calculation of the radar station field in 3D space in the presence of forest and other

obstacles by the method of parabolic equation," *2017 Progress in Electromagnetics Research Symposium* - Spring (PIERS), Russia, 22-25 May 2017.

[26] R. Janaswamy, "Path loss predictions in the presence of buildings on flat terrain: A 3-D vector parabolic equation approach," *IEEE Trans. Antennas Propag.*, vol. 51, pp. 1716-1728, 2003.

[27] W. C. Chew, *Waves and Fields in Inhomogeneous Media*. Piscataway, NJ: IEEE Press, 1995.

[28] H. F. Rasool, X. M. Pan, and X. Q. Sheng, "Radiowave propagation prediction in the presence of multiple knife edges using 3D parabolic equation method," *Proc. ACES-China*, Aug. 2018.

[29] R. Zhang, "Study on Fourier transform methods in a 3-D parabolic equation," *IEEE GASS Symposium Proc.*, 16-23 Aug. 2014.

[30] P. Suarez, "An introduction to the split step Fourier method using MATLAB," 2016. (https://doi.org/10.13140/RG.2.1.1394.0965).

[31] F. Jensen, H. Schmidt, M. B. Porter, and W. A. Kuperman, *Computational Ocean Acoustics*. 2nd ed., ser. Modern Acoustics and Signal Processing, New York, Springer-Verlag, pp. 457-530, 2011.

[32] R. H. Hardin and F. D. Tappert, "Applications of the split-step Fourier method to the numerical solution of nonlinear and variable coefficient wave equations," *SIAM Rev*., vol. 15, no. 22, p. 423, 1973.

[33] F. J. Harris, "On the use of windows for harmonic analysis with the discrete Fourier transform," *Proc. IEEE*, vol. 66, pp. 51-83, Jan. 1978.

[34] G. P. S. Cavalcante, M. A. R. Sanches, and R. A. N. Oliveira, "Mobile radio propagation along mixed paths in forest environment," *Proceedings of IMOC*, pp. 320-324, SBMO/IEEE, 1999.

[35] K. B. Thiem, "A 3D Parabolic Equation (PE) based Technique for Predicting Propagation Path Loss in an Urban Area," *Thesis and Dissertation Collection*, Naval Postgraduate School, Monterey, California, 2001.

[36] G. Liang and H. L. Bertoni, "New approach to 3-D ray tracing for propagation prediction in cities," *IEEE Trans. Antennas and Prop.*, vol. 46, no. 6, June 1998.

[37] S. Hosseinzadeh, H. Larijani, K. Curtis, A. Wixted, and A. Amini, "Empirical propagation performance evaluation of LoRa for indoor environment," *2017 IEEE 15th International Conference on Industrial Informatics (INDIN)*, Emden, Germany, 24-26 July 2017.

[38] M. West, K. Gilbert, and R.A. Sack, "A tutorial on the parabolic equation (PE) model used for long range sound propagation in the atmosphere," *Applied Acoustics*, vol. 37 pp. 31-49,1992.

[39] L. Piazzi and H. L. Bertoni, "On screen placement for building representation in Urban environments considering 2D multiple diffraction problems," *Proc. IEEE Vehicular Technology Conference*, 1999.

[40] L. Piazzi and H. L. Bertoni, "Effects of terrain on path loss in Urban environments for wireless applications," *IEEE Trans. Antennas Propag.*, vol. 46, no. 8, pp. 1138-1147, Aug. 1998.

Hafiz Faiz Rasool received his B.Sc. and M.Sc. degrees in Electronics Engineering from the Islamia University of Bahawalpur, Pakistan in 2011 and 2015, respectively. Currently, he is a full-time Ph.D. student at the School of Information and Electronics in Beijing Institute of Technology, Beijing, China. His research interest includes fast and efficient numerical algorithms in electromagnetics.

Xiao-Min Pan received his B.S. and M.S. degrees from Wuhan University (WHU), Wuhan, China, in 2000 and 2003, respectively, and the Ph.D. degree from the Institute of Electronics, Chinese Academy of Sciences, Beijing, China, in 2006. He is a Professor in the School of Information and Electronics, Beijing Institute of Technology, Beijing, China.

Xin-Qing Sheng received his B.S., M.S., and Ph.D. degrees from the University of Science and Technology of China (USTC), Hefei, China, in 1991, 1994, and 1996, respectively. He is the Chang-Jiang Professor in the School of Information and Electronics, Beijing Institute of Technology, Beijing, China.